Computers and Chemical Engineering 97 (2017) 76–84

Contents lists available at ScienceDirect

Computers and Chemical Engineering

journal homepage: www.elsevier.com/locate/compchemeng

Real time model identification using multi-fidelity models in managed pressure drilling

Ammon N. Eaton[a], Logan D.R. Beal[a], Samuel D. Thorpe[a], Casey B. Hubbell[a], John D. Hedengren[a,*], Roar Nybø[b], Manuel Aghito[b]

[a] Department of Chemical Engineering, Brigham Young University, Provo, UT, USA
[b] SINTEF Petroleum, Bergen, Norway

ARTICLE INFO

Article history:
Received 6 May 2016
Received in revised form 25 October 2016
Accepted 10 November 2016
Available online 16 November 2016

Keywords:
Drilling automation
Nonlinear model predictive control
Switched control
High fidelity control models
Managed pressure drilling

ABSTRACT

Highly accurate model predictions contribute to the performance and stability of model predictive control. However, high fidelity models are difficult to implement in real time control due to the large and often nonconvex optimization problem that must be completed within the feedback cycle time. To address this issue, a switched control scheme that uses high fidelity model predictions in real time control is presented. It uses real time simulated data to identify a linear empirical control model. The real time model identification procedure does not interrupt the process, and is suitable for nonlinear processes where offline model identification is difficult. Controller stability is discussed, and the control scheme is demonstrated in a managed pressure drilling simulation. The switched controller provides improved performance over both a high fidelity model based controller and a nonadaptive empirical model.

1. Introduction

High fidelity simulators are first principles based models that closely approximate reality, and are characterized by dynamic nonlinear equations. The most rigorous process models can contain more than 10^6 equations and variables (Pantelides et al., 2015). Such models have been used in Computational Fluid Dynamics (CFD), operator training simulators, and in process systems engineering for over 50 years (Pantelides and Renfro, 2013). Another common use for rigorous first principles models is to derive less rigorous, yet more computationally manageable, control models (Marquardt, 2001; Gonçalves et al., 2014). The value of first principles models in real time feedback control is most apparent in Model Predictive Control (MPC), which is the most widely used advanced control method in refining, chemical, and petrochemical processes (Qin and Badgwell, 2003).

Ideally, a control model would exactly describe plant dynamics in every operating condition. While this is not possible due to computational and complexity limitations, high fidelity simulators are rigorous models that accurately describe real processes over a wide range of operating conditions, thus requiring significantly less tuning from operational data than empirical models. Empirical model identification can be disruptive to operations and very costly, although this has greatly improved with closed loop identification techniques (Yan et al., 2009). Also, closed loop control systems can become unstable even with highly accurate models, and several robust control strategies have been developed to guarantee stability for linear and Nonlinear MPC (NMPC) applications (Keerthi and Gilbert, 1988; Chen and Allgöwer, 1998; Tahir and Jaimoukha, 2013; Lazar, 2006). A control model must have a certain level of accuracy before any guarantees of controller stability and performance can be made. Accurate model predictions can lead to fewer iterations because the optimizer is able to minimize the error between the process and the model more quickly than inaccurate models. If the error is inherently small, it can quickly be brought within the specified tolerance with linear or quadratic convergence rates that are typical of Sequential Quadratic Programming (SQP) solvers near the solution. Accordingly, it has been demonstrated that improved models provide better control than less rigorous models in MPC (Yip and Marlin, 2004). Additionally, many processes, such as polymer grade transitions and oil well drilling, are extremely nonlinear to the extent that linear model approximations are insufficient to control the process.

In addition to performance improvement, highly accurate model predictions allow a controller to maintain control over a process, over the prediction horizon, even when there is no process feedback due to sensor failure, etc. While sensor failure is common in oil and gas well drilling, loss of measurement

* Corresponding author.
E-mail address: john_hedengren@byu.edu (J.D. Hedengren).

http://dx.doi.org/10.1016/j.compchemeng.2016.11.008
0098-1354/

feedback is more common during normal operations due to pipe connection procedures. Maintaining control during the temporary and intermittent loss of feedback is the major motivation for using high fidelity simulators in real time control.

While high fidelity simulators have many benefits, rigorous models are difficult to implement in NMPC feedback control due to the short (typical range is 1 s to 10 min) cycle time in which a large Nonlinear Programming (NLP) problem must be solved. If the optimization is not completed within the cycle time, controller instability will occur (Santos et al., 2001; Findeisen and Allgöwer, 2004). Because of this limitation, rigorous models have not been widely implemented in real time control. However, recent improvements in algorithm design and hardware capabilities have opened up the possibility of using the accuracy of high fidelity simulators in real time feedback loops. For example, multiple control algorithms have been developed that compute the full NLP problem offline and perform only a sensitivity calculation online (Zavala and Biegler, 2009; Yang and Biegler, 2013; Pirnay et al., 2012). These sensitivity based methods have been demonstrated in controlling reactors (Zavala and Biegler, 2009), distillation columns (López-Negrete et al., 2013; Pirnay et al., 2012), power plants (López-Negrete et al., 2013), and adsorption beds (Yu and Biegler, 2015). Others have used large scale models in Dynamic Real Time Optimization (D-RTO) (Huang, 2010; Yip and Marlin, 2004; Biegler, 2009). However, this work introduces a method for using high fidelity simulators in NMPC by implementing a switched control scheme. The method uses dynamic online model assessment and control model identification from high fidelity simulated data.

2. High fidelity switched control

Switched and hybrid systems have been extensively studied (Narendra and Balakrishnan, 1997; Giovanini et al., 2014; Koutsoukos et al., 2000), and MPC variants have also been developed (Kuure-Kinsey and Bequette, 2009; Lazar et al., 2006). The formulation of stability and performance guarantees have been developed in switched linear and nonlinear MPC by several researchers (Lazar, 2006). However, none of these previous studies have attempted to incorporate high fidelity simulators into the control law to improve model predictions, and subsequently controller performance and stability. The objective of this work is to couple high fidelity model predictions with the speed and stability of linear MPC by dynamically identifying the empirical control model in a switched control scheme.

The switched controller presented in this work uses a high fidelity nonlinear, first principles based model running in parallel with the physical process. Also, a linear, empirical model predictive controller and a nonlinear model predictive controller with a simplified low order model run parallel with each other. The output suggestions of these controllers are fed into a switching algorithm that implements the linear controller suggestions into the nonlinear process. When the linear model prediction error exceeds a specified tolerance, the algorithm samples the high fidelity model with step inputs to produce a simulated data set of the current operating conditions. Then it uses regression techniques to fit the new gain and time constant in the linear, empirical model to the current simulated data set. While this model identification occurs, the algorithm implements the low order NMPC controller suggestions to maintain control over the process. Fig. 1 shows a diagram of the proposed controller scheme.

This strategy allows the slow, yet very accurate predictive capabilities of the high fidelity model to be implemented into a fast, yet locally accurate linear model, all without interrupting the process. It allows control model identification without disrupting operations. As shown in Fig. 1, this control scheme takes advantage of

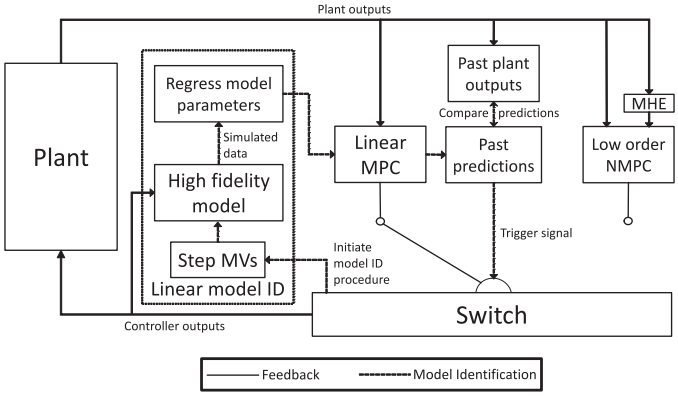

Fig. 1. Diagram of a switched control structure.

the accurate predictions of the high fidelity simulator while minimizing online computational costs. Online computation time can be further reduced by computing in parallel on separate resources.

In addition to incorporating high fidelity predictions, this switched control scheme differs from traditional gain scheduling and other switch schemes, such as Multiple Models Predictive Control (MMPC) (Kuure-Kinsey and Bequette, 2009), in that there is no predetermined switching time or sequence. Also, the control models do not need to be identified before implementing the controller. This is helpful in systems where model identification is disruptive to operations, or when identifying the model before operations begin is not possible such as with automated oil well drilling.

3. Controller stability

Even when each of the individual controllers in a switched system are asymptotically stable, destabilization due to switching among the controllers must be addressed before stability can be guaranteed (Ye et al., 1998; Liberzon and Morse, 1999). Therefore, it is necessary that the switch itself and the individual controllers are stable. For implementation of the present switched control algorithm, the individual MPC controllers can be formulated to take advantage of the recent advances in NMPC stability theory found in Mayne (2014) and the included citations. In essence, stability can be achieved if a feasible solution is found and the finite optimization horizon is sufficiently long. Methods exist to efficiently calculate the horizon length required for stability to be ensured at each time step (Pannek and Worthmann, 2014). Other methods require the addition of terminal cost constraints or a continuous Lyapunov function. Yet, these stability methods are insufficient for hybrid systems because of the discontinuous derivatives associated with switching (Lazar, 2006). The stability of this switching algorithm is addressed in a way that is unique to this control scheme.

Stability of switched and hybrid MPC systems has been centered around piecewise affine systems (Magni et al., 2008; Lazar, 2006). In other words, switched piecewise affine systems, such as MMPC or Switched MPC (S-MPC), switch among controllers with locally affine regions. The switching is from a locally accurate controller to a neighboring locally accurate controller (Mayne, 2014). In contrast, this work presents a scheme that switches among NMPC controllers that are accurate in the same operating regions. This redundant control model structure has several benefits including online model maintenance and some desirable stability properties. For instance, one of the major issues with discontinuous switching of redundant continuous NMPC controllers is the jump in controller outputs that can occur upon switching (Eaton et al., 2015). This sudden change in process inputs can result in poor or lost control. This jump occurs because the individual NMPC optimizers can find local minima of a nonconvex problem resulting in

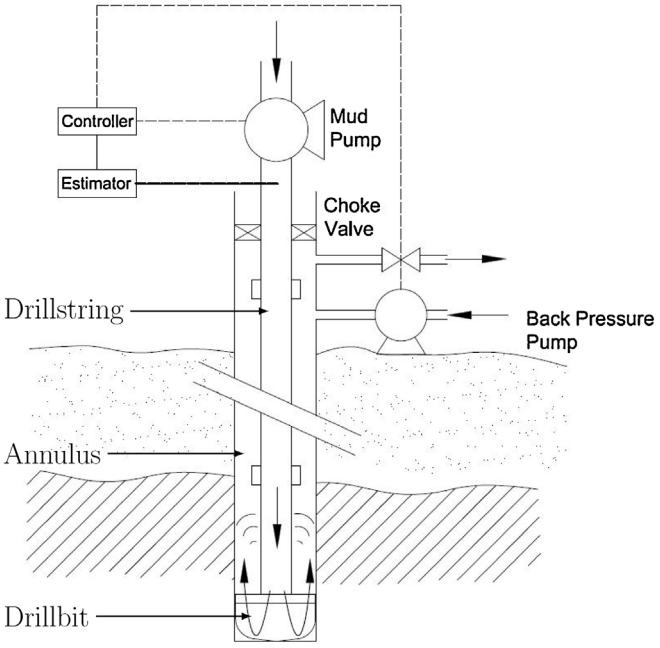

Fig. 2. Simplified schematic of the automated MPD process.

differing manipulated variable (MV) suggestions to achieve the same controlled variables (CVs). Factors such as MV move suppression or the multivariate nature of the problem contribute to this discontinuity between MV suggestions to reach the same CV targets. When switching among controller suggestions, the undesirable jump is manifest. One of the contributions of this work is addressing switch stability by synchronizing the NMPC controllers. This is accomplished by initializing each of the NMPC optimization problems, at each time step, with the current process conditions. Because each controller starts with the same initial conditions, and use the same optimization routine, each converges to similar solutions and transitions between solutions are smooth. Also, the switching is induced when past control model predictions no longer match past process measurements within a specified accuracy. This means that switching between controllers will only occur if it stabilizes the system. After a switch is made, another switch cannot occur for a given "dwell time", this prevents instability associated with switch chatter (Shorten et al., 2007). With the assumption that the individual controllers are stable, and combined with the previously stated synchronization techniques, switch stability is implied.

4. Simulated managed pressure drilling

The switched control strategy is demonstrated on a simulated oil well drilling process. An oil well is created by drilling into the earth for several hundred to several thousand feet, stopping to insert and cement casing pipe to the well bore, then repeating the process until the target depth is reached. As the well deepens, more drill pipe is connected to the drillstring. At the bottom of the drillstring, a Bottom Hole Assembly (BHA), consisting of measurement and steering equipment, is attached to the drill bit. The drill bit is cooled by the drilling fluid, or mud, which also moves the rock cuttings to the surface and maintains pressure in the well annulus (see Fig. 2). The well annulus fluid pressure consistently needs to be greater than the geologic reservoir fluid pressure to prevent hydrocarbons from entering the well during the drilling process. If the mud pressure in the well is too high it can damage the rock formation; if it is too low hydrocarbons from the subsurface reservoir can come to the surface in an uncontrolled and dangerous manner. When this catastrophe happens it is known as a blowout. The well bore pressure must be maintained within a small range of pressures that will balance the reservoir fluid pressure to prevent fractured formations and blowouts. To help achieve this pressure balance, a variation of traditional drilling, called Managed Pressure Drilling (MPD), was developed. A simplified schematic of MPD is shown in Fig. 2. MPD uses pressure measurements from the BHA to inform the driller of the need to adjust the main mud pump flow rate and choke valve opening to reach the desired pressure target in the well. A back pressure pump is used to maintain well pressure during pipe connection procedures when the main mud pump is disconnected from the drillstring.

Automation of MPD is advancing in industrial practice with mass balance control of the drilling mud being the most common practice. Another automated MPD method takes advantage of a highly calibrated high fidelity simulator whose predictions are used as feedback for a controller which manipulates the choke valve to control the bit pressure in the real process (Bjørkevoll et al., 2010). It has also been demonstrated that an automated controller can maintain borehole pressure and reject disturbances faster and more accurately than manual control by using NMPC with high quality process data (Asgharzadeh Shishavan et al., 2015). One of the major challenges with implementing NMPC is the quality of the data sent by the downhole instruments. The most common method of receiving continual pressure measurement data from the BHA is through mud pulsing (Veeningen, 2011). In mud pulsing, a pressure transducer sends pressure waves through the annulus fluid to a receiver at the surface. The pulses are then decoded into pressure measurements. Currently, the maximum data transmission rate of mud pulsing is 80 bits per second (Asgharzadeh Shishavan et al., 2014). One of the major limitations of mud pulsing technology is the need to have the mud flowing for it to work. This makes receiving downhole pressure measurements impossible when the mud pump stops for regular events such as pipe connection procedures. Additionally, the small bandwidth and long delay time of mud pulsing technology pose a significant challenge to automating MPD with direct downhole pressure measurements, and improving the technology is an active area of research (Zhidan et al., 2015). Other researchers are moving away from mud pulsing in favor of other technologies such as Wired Drill Pipe (WDP) (Veeningen, 2011). Regardless of the means of transmission, the downhole data quality is substantially low ($\pm$20 bar) for traditional sensors and better ($\pm$1 bar) for newer sensors (Openfield Technology, 2015) that have been developed to meet MPD control requirements. Even with the new pressure sensors, the inherently harsh borehole environment and the discontinuous nature of the drilling process make data collection and reliability a challenge.

Additionally, several abnormal events can occur during drilling operations. For example, drilling into an unexpected high pressure reservoir can offset the well/reservoir pressure balance and allow an unwanted influx of gas into the well bore. This situation is known as unwanted gas influx or kick, and is characterized by an increase in pressure in the annulus as the gas rises to the surface and increased flow rate in the annulus that acts as a disturbance to the process. In practice, the drilling process is stopped and shut in until the gas is circulated out and the well is controlled with a change in mud weight or choke valve position. In automated MPD, the set point for the choke pressure is increased to stop the influx of gas. Then, drilling operations are slowly brought online after the mud density is increased sufficiently to balance the new pressure at the bit. Controlling a kick is known as well control, and is an active area of research in industry and academia. Kicks, pipe connection procedures, delayed bit pressure measurements, and measurement noise are all factors included in the simulation to better simulate issues encountered in industrial practice.

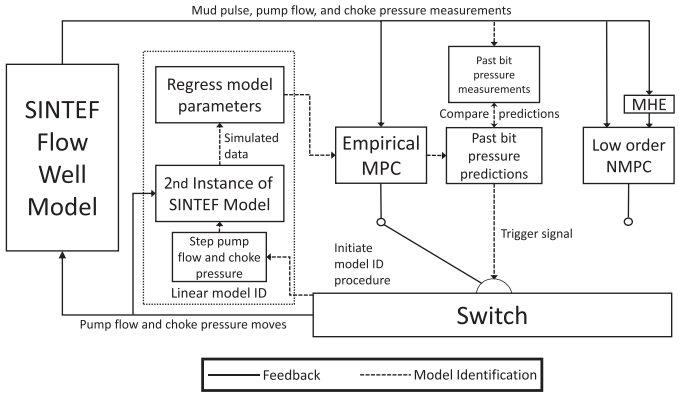

Fig. 3. Diagram of the switched control structure used in this work.

In these simulations, the mud pump flow rate and choke pressure are the MVs and the CV is the pressure at the bottom of the well. As the drill bit is always at the bottom of the well, the bit pressure is used for the CV. An empirical model and a low order first principles model are used in parallel MPC controllers as depicted in Fig. 3. These controllers are described in Sections 4.1 and 4.2.

4.1. Empirical controller

The empirical controller model uses a linear First Order Plus Dead Time (FOPDT) model, as seen in Eq. (1), with gain (κ), time constant (τ), and dead time (θ) that are fit to simulated data from the SINTEF Flow Model high fidelity simulator (Petersen et al., 2008) in the procedure described in Section 3. The simulated data are generated by artificially stepping each of the MVs up and down in slow succession across prescribed operating ranges.

$$\tau \frac{dx}{dt} = -x + \kappa u(t-\theta) \tag{1}$$

In Eq. (1), x represents the bit pressure (P_{bit}) and u is a vector representing the mud pump flow rate (q_{pump}) and the pressure upstream of the choke valve (P_{choke}) which are model inputs. Once the individual input/output relationships are established, they are concatenated into a single matrix. This matrix is used to generate a state space model for the Multiple Input Single Output (MISO) MPD process controller at each identification routine. The MPC controller uses an ℓ_1-norm objective function that allows the formulation of a dead-band region for the set point, rather than one specific target value. Eq. (2) shows the generalized ℓ_1-norm control formulation.

$$\begin{aligned}
\min_{x,y,u} \Phi \quad &= w_{hi}^T e_{hi} + w_{lo}^T e_{lo} + y^T c_y + u^T c_u + \Delta u^T c_{\Delta u} \\
\text{s.t.} \quad & 0 = f\left(\frac{dx}{dt}, x, y, p, u\right) \\
& 0 = g(x, y, p, u) \\
& 0 \le h(x, y, p, u) \\
& \tau_c \frac{dy_{t,hi}}{dt} + y_{t,hi} = sp_{hi} \\
& \tau_c \frac{dy_{t,lo}}{dt} + y_{t,lo} = sp_{lo} \\
& e_{hi} \ge y - y_{t,hi} \\
& e_{lo} \ge y_{t,lo} - y
\end{aligned} \tag{2}$$

In this formulation, Φ is the objective function, x, y, and u are vectors of the process states, the model predictions, and the model inputs respectively. In the MPD case, u would be a vector of the mud flow rate and choke pressure, y would equal x and be the bit pressure. w_{hi} and w_{lo} are penalty matrices for solutions outside of the dead-band region, while e_{hi} and e_{lo} are slack variables for the dead-band high and low limits. c_y, c_u, and $c_{\Delta u}$ are cost vectors for the model predictions, inputs, and change of inputs respectively. f is a generalized function of the model equations as functions of x, y, u, p and dx/dt, where dx/dt is the time derivative of x and p is a vector of the model parameters. Similarly, g is a generalized function of the system equality constraints, and h is a generalized function of the systems inequality constraints. τ_c is the desired CV time constant, and $y_{t,hi}$ and $y_{t,lo}$ are the upper and lower limits of the desired trajectory when changing set points. sp_{hi} and sp_{lo} define the set point dead-band region. The controller is tuned by adjusting the weighting vectors: c_y, c_u, $c_{\Delta u}$, w_{hi}, and w_{lo}, and the CV time constant τ_c. The tuning favors adjusting the choke pressure as much as possible before the pump is adjusted to reach the set point. This is because the pump needs a flow rate sufficient to remove rock cuttings up the annulus. A sudden drop in mud flow can cause the solids in the annulus to precipitate and lead to an expensive and disruptive stuck pipe situation. Unnecessary control moves are further mitigated by the dead-band region set point.

Within the dead-band region (between upper and lower limits) there is no penalty in the objective function. The use of a dead-band helps reject noise and mitigate unnecessary control moves (Hedengren and Eaton, 2015), helping extend the life of equipment and avoiding actions that vigilant operators would find unnecessary. The absolute value of the error is also implemented in a unique way to avoid the discontinuous first derivative of the objective function (which is inherent to an absolute value function), improving the effectiveness of gradient based solution techniques such as SQP. Further details on the formulation and implementation of this ℓ_1-norm dead-band objective function are found in Hedengren et al. (2014).

Table 1
Description of variables and parameters used in the low order drilling model with initial values.

Variable	Definition	Initial value
P_p	Main pump pressure (state variable – SV)	86 $\text{bar}_{\text{gauge}}$
β_d	Bulk modulus of the drillstring	14,000 $\text{bar}_{\text{gauge}}$
V_d	Volume of the drillstring	19.909 m^3
q_{pump}	Flow rate of the main pump	1.8 m^3/min
q_{bit}	Flow rate of the fluid through the drill bit (SV)	1.8 m^3/min
P_c	Choke valve pressure (SV)	52 $\text{bar}_{\text{gauge}}$
β_a	Bulk modulus of the annulus	14,000 $\text{bar}_{\text{gauge}}$
V_a	Volume of the annulus	13.3515 m^3
q_{back}	Back pressure pump flow rate	0 m^3/min
q_{choke}	Choke valve flow rate	1.8 m^3/min
q_{res}	Reservoir gas influx flow rate	0 m^3/min
M	Effective density per unit length	3500 kg m^{-4} $10e^{-5}$
M_a	Effective density per unit length of annulus	800 kg m^{-4} $10e^{-5}$
M_d	Effective density per unit length of drillstring	2700 kg m^{-4} $10e^{-5}$
f_d	Friction coefficient of drillstring	1 bar s^2 m^{-6}
f_a	Friction coefficient of the annulus	623.87 m^{-5}
ρ_d	Actual density in the drillstring	1490 kg m^{-3}
ρ_a	Actual density in the annulus	1372.1 kg m^{-3}
g	Gravitational constant	9.81 m s^{-2}
P_{bit}	Pressure at the bit	440 $\text{bar}_{\text{gauge}}$
h_{bit}	Well depth	2150 m
P_0	Pressure at the surface	1 $\text{bar}_{\text{absolute}}$

4.2. Low order controller

The low order controller uses a reduced order observer model developed by Stamnes et al. (2008), adapted for WDP control by Asgharzadeh Shishavan et al. (2014), and further modified for mud pulse telemetry in this work as shown in Eqs. (3)–(8). Descriptions of the model variables and parameters are shown in Table 1.

$$P_{bit} = P_c + \rho_a f_a h_{bit} (q_{bit})^2 + \rho_a g h_{bit} \tag{3}$$

$$q_{choke} = K_c Z_{choke} [\rho_a (P_c - P_o)]^{0.5} \tag{4}$$

$$\frac{dP_c}{dt} = \frac{\beta_a}{V_a}(q_{bit} + q_{back} - q_{choke} + q_{res}) \tag{5}$$

$$\frac{dq_{bit}}{dt} = \frac{1}{M}(P_p - f_d q_{bit}^2 + \rho_d g h_{bit} - P_{bit}) \tag{6}$$

$$\frac{dP_p}{dt} = \frac{\beta_d}{V_d}(q_{pump} - q_{bit}) \tag{7}$$

$$M = M_a + M_d \tag{8}$$

The low order MPC controller also uses the ℓ_1-norm objective function formulation used by the empirical MPC controller. This controller was tuned by adding a cost for changing the valve position and pump flow rate, and limiting the amount the controller moves these variables at each time in the control horizon. Also, the density of the mud in the annulus and the annulus friction factor are changing as rock cuttings are carried away during drilling. These two parameters are required inputs to the model and need to be estimated because they cannot be measured. Therefore, the controller is combined with online Moving Horizon Estimation (MHE), which uses a similar ℓ_1-norm objective function, to estimate the annulus friction factor and density in the annulus at each time step. The estimator uses the same low order model described above. Eq. (9) shows the objective function, slack variables, and error equations for the MHE used in this work.

$$\begin{aligned}
\min_{x,y,p} \Phi \quad &= w_m^T(e_U + e_L) + w_p^T(c_U + c_L) + \Delta p^T c_{\Delta p} \\
\text{s.t.} \quad & 0 = f\left(\frac{dx}{dt}, x, y, p, u\right) \\
& 0 = g(x, y, p, u) \\
& 0 \le h(x, y, p, u) \\
& e_U \ge y - y_x + \frac{db}{2} \\
& e_L \ge y_x - \frac{db}{2} - y \\
& c_U \ge y - \hat{y} \\
& c_L \ge \hat{y} - y \\
& e_U, e_L, c_U, c_L \ge 0
\end{aligned} \tag{9}$$

Here, p is a vector of the model parameters that are estimated, w_m is a cost given for measurement deviation, w_p is a cost given for deviation from the previous solution, and Δp is the change in model parameters. e_U and e_L are slack variables for the dead-band upper and lower limits, c_U and c_L are slack variables for the upper and lower limits of the prior model solution, and $c_{\Delta p}$ is a cost for changing the previous parameter values. Also, y_x is a vector of process measurements, db is the size of the dead-band, and $\hat{y}$ is the previous model values. A more complete presentation of the estimation form of the ℓ_1-norm objective function is found in Hedengren et al. (2014). While the ℓ_1-norm objective function has many advantages, one of the shortcomings is the lack of developed theory concerning the estimated parameter nonlinear confidence bands and noise covariance (Safdarnejad et al., 2016). It is not within the scope of this work to develop this theory, but it should be noted that the nonlinear parameter confidence regions are considered in this work. The measurement variance is addressed by setting the dead-band region at approximately the same size as the bit pressure measurement noise in the system. This prevents the signal noise from significantly influencing the parameter estimates, only when there is a shift outside the predicted dead-band zone. This practical approach assumes that the parameter estimates are sufficiently accurate when the predicted bit pressure remains within the dead-band region.

4.3. Controller switch

The switch in this simulation uses the logic described in Section 4. Specifically, prior linear model predictions are compared to physical process outputs over a horizon of 20 time steps at each instance. When the bit pressure predictions exceed an absolute error of 1.7 bar, the low order NMPC controller is implemented in the feedback loop, and the linear model tuning procedure is initiated as described in Section 4.3.1. The past prediction horizon and the acceptable prediction error are tuning parameters for this controller. Also, if the MPC optimization solution is infeasible or not convergent for both controllers, then the switch defaults to the empirical controller as the probability of convergence is greater for this controller.

4.3.1. Dynamic model identification

In the real time model identification procedure, the switch triggers the high fidelity model to simulate the well at the current conditions. The mud pump flow rate is perturbed in a doublet test (up, down, back to nominal conditions) to generate simulated dynamic data from the high fidelity simulator. In this particular application, the simulated step test covers a 12 time step horizon. This is repeated for the choke pressure, and then the simulated data is used to regress the empirical model parameters. Fig. 4 shows the step in MVs and the response of the CV for the model identification procedure. Fig. 4 also shows the fit of the model parameters to the simulated data for a typical online model identification procedure. Fig. 4 is representative of a typical fitting procedure; however, each fitting instance will vary slightly from the results in this figure. Once the new model parameters are identified, they are sent to the controller, and the switch continues to monitor the accuracy of the model predictions for at least 5 time steps before another switch can be made. This dwell time prevents switch chatter and the instabilities associated with it. In this work, it is assumed that the high fidelity model parameters are accurate and do not require updating in the time scales of these simulations. In longer times scales, such as industrial application, high fidelity parameter model parameters should also be updated.

4.4. Oil well drilling process

The drilling process is simulated using the SINTEF Flow Model high fidelity simulator (Petersen et al., 2008) as the plant. A separate instance of the model is used for tuning the linear model. The model parameters that are clearly known *a priori*, such as drill bit

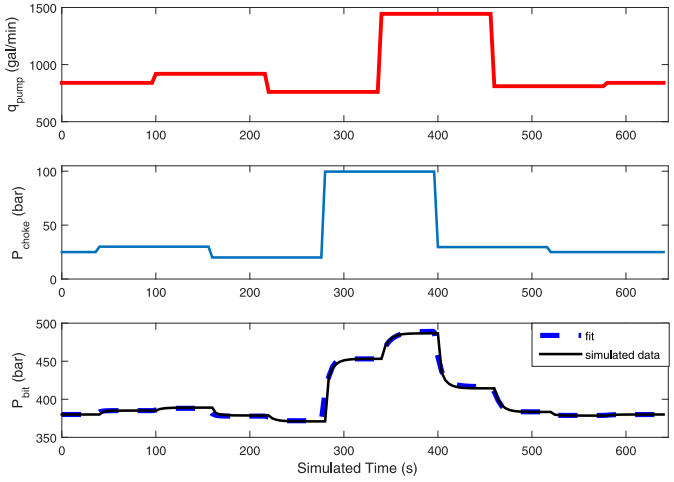

Fig. 4. Simulated step test, system response, and resulting fit for the empirical model identification.

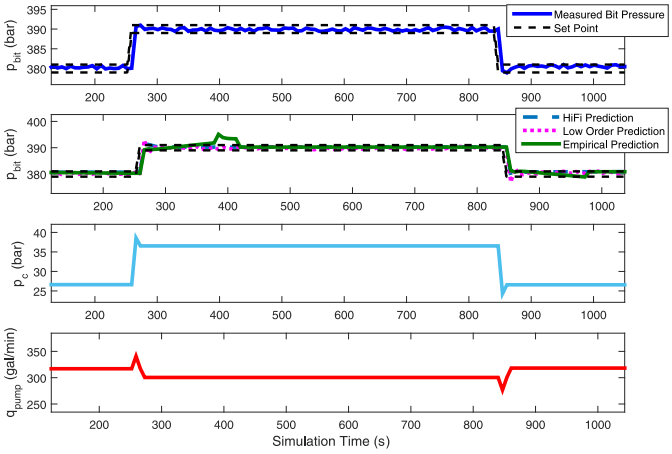

Fig. 5. Switched controller response to set point changes in bit pressure (P_{bit}).

diameter and density of the mud in the drillstring, are identical in each instance of the model. However, unknown variables, such as reservoir depth and rock type, and formation pressure are set to different values in the tuning model. This ensures that the model predictions do not contain information that would not be known in practice. Additionally, the low order and empirical control models are updated with current well information through feedback of the bit pressure. The rate of penetration (ROP) is held constant at 6.5 ft/h in the vertical well, and dynamic temperature effects are not included in the simulations.

4.5. Simulation results and discussion

Two common drilling scenarios are simulated including normal drilling and unwanted gas influx (kick). The results of these simulations are found in Sections 4.5.1 and 4.5.2 respectively.

4.5.1. Normal drilling operations

In this simulation, the controller receives measurements from the well every 7 s. Fig. 5 shows the results of the continuous drilling simulation with set point changes. The bit pressure set point for this simulation is 380 bar. At 300 s the set point is adjusted to 390 bar and then back to 380 bar at 840 s. The top plot of Fig. 5 shows the bit pressure remains within the dead band set point region even when the empirical control model parameters are being identified and the low order model is implemented in the feedback loop. The switching between the controllers results in bumpless control. The third and fourth subplots show the movements of the choke pressure and the mud pump flow rate respectively. As seen in the top plot, the controller keeps the bit pressure within the set point range. The second plot shows the individual controller predictions, and at about 370 s the empirical controller predictions exceed the acceptable limit. This initiates the tuning procedure. The switching and tuning occurs once again at 966 s after the set point change. The switching and tuning does not happen during the set point changes indicating that the loss of control from the empirical model is not due to poor tuning. It is interesting to note that the high fidelity predictions and the empirical model predictions are identical except when the process dynamics change and the empirical model is unable to maintain control. Once the model identification process is complete, the empirical model predictions match the high fidelity model once again. This demonstrates that the control scheme effectively incorporates the high fidelity model predictions into real time control.

Fig. 6 shows the time of switching between controllers in the top plot, and a comparison of real time and simulation time in the bottom plot. As long as the bottom plot is less than one, as denoted

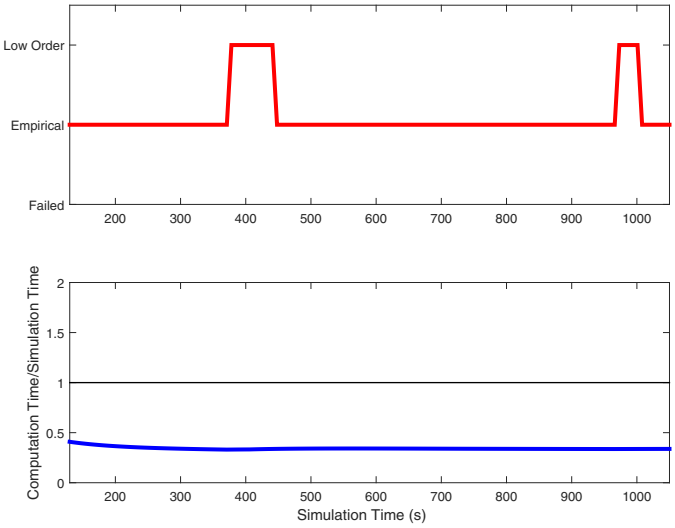

Fig. 6. Controller switching times and computation time. When the Computation Time/Simulation Time is below the line at 1 on the vertical axis, the computation occurs in real time.

by the black horizontal line, the computation time is faster than real time, and the controller will complete the necessary calculations within the feedback cycle time.

To contrast the switched control scheme, Fig. 7 shows the results of an NMPC controller using the high fidelity model directly in the optimization routine. Due to the format of the high fidelity simulator used, this NMPC controller used a shooting method to solve the optimization problem. The control horizon was 4 s and was solved using the IPOPT (Wächter and Biegler, 2006) solver option in the *fmincon* function in MATLAB. The controller clearly maintains the bit pressure in the set point region demonstrating very good control.

Fig. 8 shows a comparison of actual time and simulation time for this simulation, and it is clear that the computation time at each control cycle is too long for real time implementation. This simulation justifies the complexity of this switched control scheme. It implements the accuracy of the high fidelity model for control with significantly reduced computation within the feedback cycle time.

4.5.2. Unexpected gas influx

The controller is used in a simulated disturbance rejection scenario. Unexpected gas influx from the reservoir into the well bore is

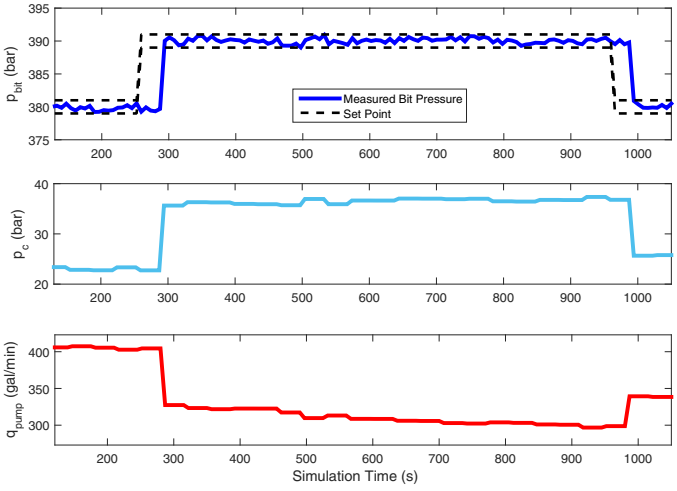

Fig. 7. MPD control using only a high fidelity control model.

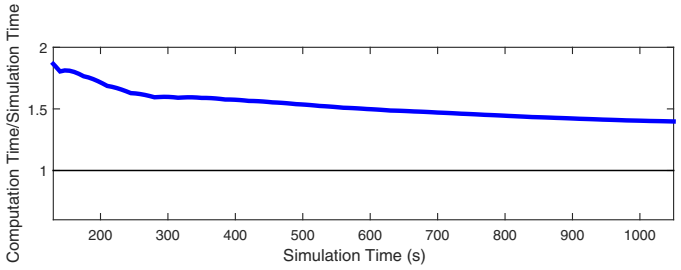

Fig. 8. High fidelity controller computation time. When the Actual Time/Simulation Time is below the line at 1 on the vertical axis, the computation occurs in real time. This controller could not be implemented in real time.

Table 2
Values of key variables used in the gas influx simulation.

Variable	Values at 130 s of simulation time
Mud pump flow rate	393.6 gal/min
Choke pressure	22.5 bar_{gauge}
Reservoir depth	7874.5 ft
Mud density	11.7 lbs/gal
Bit pressure	378.7 bar_{gauge}
Well trajectory	Vertical
Well depth (TVD)	7874.2 ft
ROP	6.5 ft/h
Kick size	30 bbls
Sample rate	10 s

a common occurrence in drilling. In this simulation the drill bit suddenly hits an unexpected high pressure zone. When this happens, the high pressure reservoir gas disrupts the well pressure balance. Table 2 shows the conditions for this simulation at 130 s when the time of interest begins.

Fig. 9 demonstrates the controller response to this moderate kick. The top subplot of Fig. 9 shows the controller effectively maintains the bit pressure within the specified set point in the presence of a process disturbance. The kick begins at about 300 s and continues throughout the remainder of the simulation (see Fig. 9). The dashed black lines in Fig. 9 denote the set point region. When the bit pressure is within these lines, the controller takes no corrective actions. There is a small (<2 bar) increase in bit pressure when the kick occurs due to the sudden increase in reservoir pressure encountered by the bit. This pressure increase moves the bit pressure slightly outside of the set point region (at 310 s) and provokes a response from the controller as seen in Fig. 10. Because the mud is oil based and under high pressure, the gas easily dissolves into the

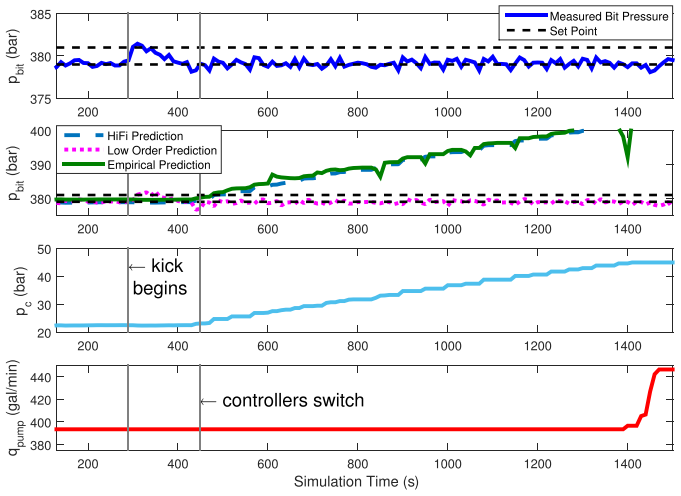

Fig. 9. Controller response to a process disturbance of unwanted gas influx.

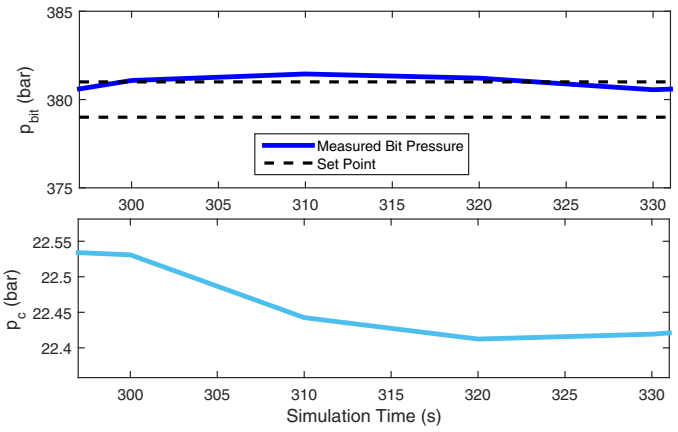

Fig. 10. Controller response to a set point violation that occurs at the onset of the kick.

fluid which decreases the density of the mud and, consequently, the hydrostatic pressure of the mud. This brings the bit pressure down even though there is little change in the choke pressure or the mud flow. When the bit pressure drops below the set point region at 420 s, the controller increases the choke pressure slightly until 450 s when a switch is made to the low order controller for the remainder of the simulation. The controller continues to increase the choke pressure, and eventually the mud flow, because the addition of dissolved gas into the mud column continues to lower the hydrostatic pressure on the bit.

It is interesting to note that the low order controller is used for disturbance rejection as seen in Fig. 9. This is because the high fidelity model parameters are not updated by changing process conditions, and it does not account for the disturbance in its predictions. Consequently, the predicted bit pressure is too high and it tunes the empirical model accordingly (see the second subplot in Fig. 9). At several instances the empirical controller attempts to minimize the error between the predicted bit pressure and the set point, yet as the initial error is greater than the switching tolerance, the controller tunes the empirical model back to the high fidelity model. This continues until the high fidelity model parameters are updated. Meanwhile, the low order controller is updated by the process, and it is able to keep the bit pressure within the acceptable range. The third subplot in Fig. 9 shows the choke pressure progressively increases until it reaches the upper limit of 45 bar. At this point (about 1400 s) the choke pressure can no longer be

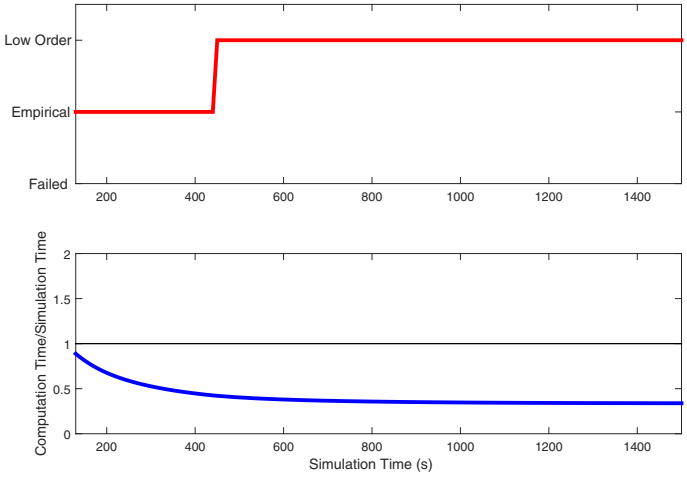

Fig. 11. Controller switching and simulation time.

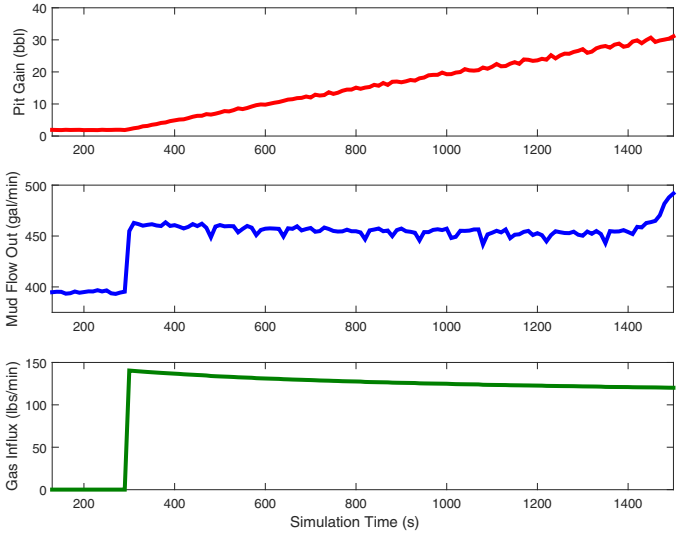

Fig. 12. Pit gain, choke flow, and gas influx rate for the kick simulation.

used to maintain the bit pressure and the previously constant mud pump increases flow to compensate.

Fig. 11 shows the controller switching and also a comparison of simulation time and real time to demonstrate the controller can be used in real time. As long as the bottom plot of Fig. 11 is less than one, the controller will complete the computations within the required feedback cycle times, and the controller will be stable.

Fig. 12 shows the drilling mud pit gain, flow through the choke, and the simulated gas influx from the reservoir to the well bore. The sudden increase in pit gain and choke flow are primary signs that a kick is occurring. In a real situation the drilling crew would stop the process and implement the appropriate well control procedures.

5. Conclusion

A switched control scheme is presented that makes use of a high fidelity model running in parallel with a process. The high fidelity model is used to generate simulated data to identify the model parameters of a linear empirical control model in MPC. During the model identification procedure, the switch implements a low order control model to control the process. In this way the model identification procedure does not disrupt the controller. The model identification procedure is triggered when the error in the past predictions of a linear model exceeds a prescribed threshold. The switched control scheme allows the highly accurate predictions of a high fidelity model to be incorporated in real time control without the high online computational cost. The control scheme is applied to a simulated managed pressure drilling process. The controller performance is demonstrated under set point tracking and disturbance rejection scenarios. Future work on the control scheme includes updating the high fidelity model parameters with process data with moving horizon estimation, and controlling a process when feedback is lost and highly accurate model predictions are necessary.

Acknowledgments

This work has been carried out as part of the research project Improved Model Support in Drilling Automation, financed by Huisman Equipment and the Research Council of Norway. The authors would also like to thank Huisman for valuable feedback during the writing process.

References

Asgharzadeh Shishavan, R., Hubbell, C., Perez, H., Hedengren, J.D., Pixton, D., Craig, A., 2014. Addressing UBO and MPD challenges with wired drill pipe telemetry and model predictive control. In: SPE/IADC Managed Pressure Drilling and Underbalanced Operations Conference.

Asgharzadeh Shishavan, R., Hubbell, C., Perez, H., Hedengren, J.D., Pixton, D., 2015. Combined rate of penetration and pressure regulation for drilling optimization by use of high-speed telemetry. SPE Drill. Complet. J. 30 (1), 17–26.

Biegler, L.,2009. Technology advances for dynamic real-time optimization. In: 10th International Symposium on Process Systems Engineering: Part A, vol. 27 of Computer Aided Chemical Engineering. Elsevier, pp. 1–6.

Bjørkevoll, K.S., Hovland, S., Aas, I.B., Vollen, E., 2010. Successful use of real time dynamic flow modelling to control a very challenging managed pressure drilling operation in the north sea. In: SPE/IADC Managed Pressure Drilling and Underbalanced Operations Conference and Exhibition.

Chen, H., Allgöwer, F., 1998. A quasi-infinite horizon nonlinear model predictive control scheme with guaranteed stability. Automatica 34, 1205–1217.

Eaton, A., Beal, L., Thorpe, S., Janis, E., Hubbell, C., Hedengren, J., Nybø, R., Aghito, M., Bjørkevoll, K., Boubsi, R.E., Braaksma, J., van Og, G., 2015. Addressing discontinuous process challenges with multi-fidelity model predictive control. In: AIChE Annual Meeting, Salt Lake City, UT.

Findeisen, R., Allgöwer, F., 2004. Computational delay in nonlinear model predictive control. In: Proc. Int. Adv. Control of Chemical Processes, ADCHEM'03, Hong Kong.

Giovanini, L., Sanchez, G., Benosman, M., 2014. Observer-based adaptive control using multiple-models switching and tuning. IET Control Theory Appl. 8 (4), 235–247.

Gonçalves, G.A., Secchi, A.R., E.C.B. Jr.,2014. Fast nonlinear predictive control and state estimation of distillation columns using first-principles reduced-order model. In: 24th European Symposium on Computer Aided Process Engineering, vol. 33 of Computer Aided Chemical Engineering. Elsevier, pp. 715–720.

Hedengren, J.D., Eaton, A.N., 2015. Overview of estimation methods for industrial dynamic systems. Optim. Eng., 1–24.

Hedengren, J.D., Shishavan, R.A., Powell, K.M., Edgar, T.F., 2014. Nonlinear modeling, estimation and predictive control in APMonitor. Comput. Chem. Eng. 70, 133–148.

Huang, R., 2010 12. Nonlinear Model Predictive Control and Dynamic Real Time Optimization for Large-Scale Processes. Carnegie Mellon University (Ph.D. thesis).

Keerthi, S., Gilbert, E., 1988. Optimal infinite-horizon feedback laws for a general class of constrained discrete-time systems: stability and moving-horizon approximations. J. Optim. Theory Appl. 57, 265–293.

Koutsoukos, X., Antsaklis, P.J., Stiver, J., Lemmon, M., 2000. Supervisory control of hybrid systems. Proc. IEEE 88 (7), 1026–1049.

Kuure-Kinsey, M., Bequette, B., 2009. Multiple model predictive control of nonlinear systems. In: Magni, L., Raimondo, D., Allgöwer, F. (Eds.), Nonlinear Model Predictive Control, vol. 384 of Lecture Notes in Control and Information Sciences. Springer, Berlin/Heidelberg, pp. 153–165.

López-Negrete, R., D'Amato, F.J., Biegler, L.T., Kumar, A., 2013. Fast nonlinear model predictive control: formulation and industrial process applications. Comput. Chem. Eng. 51, 55–64.

Lazar, M., Heemels, W., Weiland, S., Bemporad, A., 2006. Stabilizing model predictive control of hybrid systems. IEEE Trans. Autom. Control 51 (11), 1813–1818.

Lazar, M., 2006. Model Predictive Control of Hybrid Systems: Stability and Robustness. Eindhoven University of Technology (Ph.D. thesis).

Liberzon, D., Morse, A.S., 1999. Basic problems in stability and design of switched systems. IEEE Control Syst. Mag., 59–70.

Magni, L., Scattolini, R., Tanelli, M., 2008. Switched model predictive control for performance enhancement. Int. J. Control 81 (12), 1859–1869.

Marquardt, W., 2001. Nonlinear model reduction for optimization based control of transient chemical processes. In: Rawlings, J.B., Ogunnaike, B.A., Eaton, J.W. (Eds.), Chemical Process Control VI. Tucson, Arizona, pp. 12–42.

Mayne, D.Q., 2014. Model predictive control: recent developments and future promise. Automatica 50 (12), 2967–2986.

Narendra, K., Balakrishnan, J., 1997. Adaptive control using multiple models. IEEE Trans. Autom. Control 42 (2), 171–187.

Openfield Technology, 2015. Micropressure and Temperature Digital Sensor for OEM Integration, Brochure. http://openfield-technology.com/wp-content/uploads/2012/04/OpenFieldBrochure_OEM_recorderLight.pdf.

Pannek, J., Worthmann, K., 2014. Stability and performance guarantees for model predictive control algorithms without terminal constraints. ZAMM – J. Appl. Math. Mech./Z. Angew. Math. Mech. 94 (4), 317–330.

Pantelides, C., Renfro, J., 2013. The online use of first-principles models in process operations: review, current status and future needs. Comput. Chem. Eng. 51, 136–148.

Pantelides, C., Nauta, M., Matzopoulos, M., 2015. Equation-oriented process modelling technology: recent advances and current perspectives. In: 5th Annual TRC-Idemitsu Workshop.

Petersen, J., Rommetveit, R., Bjørkevoll, K.S., Frøyen, J., 2008. A general dynamic model for single and multi-phase flow operations during drilling, completion, well control and intervention. In: IADC/SPE Asia Pacific Drilling Technology Conference and Exhibition.

Pirnay, H., López-Negrete, R., Biegler, L.T., 2012. Optimal sensitivity based on IPOPT. Math. Program. Comput. 4 (4), 307–331.

Qin, S.J., Badgwell, T.A., 2003. A survey of industrial model predictive control technology. Control Eng. Pract. 11 (7), 733–764.
Safdarnejad, S.M., Gallacher, J.R., Hedengren, J.D., 2016. Dynamic parameter estimation and optimization for batch distillation. Comput. Chem. Eng. 86, 18–32.
Santos, L.O., Afonso, P.A., Castro, J.A., Oliveira, N.M., Biegler, L.T., 2001. On-line implementation of nonlinear MPC: an experimental case study. Control Eng. Pract. 9 (8), 847–857.
Shorten, R., Wirth, F., Mason, O., Wulff, K., King, C., 2007. Stability criteria for switched and hybrid systems. SIAM Rev. 49 (4), 545–592.
Stamnes, Ø., Zhou, J., Kaasa, G.-O., Aamo, O.M., 2008. Adaptive observer design for the bottomhole pressure of a managed pressure drilling system. In: IEEE Conference on Decision and Control.
Tahir, F., Jaimoukha, I.M., 2013. Causal state-feedback parameterizations in robust model predictive control. Automatica 49 (9), 2675–2682.
Veeningen, D., 2011. Along-string pressure evaluation enabled by broadband networked drillstring provide safety, efficiency gains. In: Offshore Technology Conference.
Wächter, A., Biegler, L.T., 2006. On the implementation of an interior-point filter line-search algorithm for large-scale nonlinear programming. Math. Program. 106 (1), 25–57.
Yan, J., Harinath, E., Dumont, G., 2009. Closed-loop identification for model predictive control: direct method. In: Decision and Control, 2009 Held Jointly with the 2009 28th Chinese Control Conference. Proceedings of the 48th IEEE Conference on CDC/CCC 2009, pp. 2592–2597.
Yang, X., Biegler, L.T., 2013. Advanced-multi-step nonlinear model predictive control. J. Process Control 23 (8), 1116–1128.
Ye, H., Michel, A.N., Hou, L., 1998. Stability theory for hybrid dynamical systems. IEEE Trans. Autom. Control 43 (4), 461–474.
Yip, W.S., Marlin, T.E., 2004. The effect of model fidelity on real-time optimization performance. Comput. Chem. Eng. 28, 267–280.
Yu, M., Biegler, L., 2015. Nonlinear model predictive control of a bubbling fluidized bed adsorber for post-combustion carbon capture. In: AIChE Annual Meeting, Salt Lake City, UT.
Zavala, V.M., Biegler, L.T., 2009. The advanced-step NMPC controller: optimality, stability and robustness. Automatica 45 (1), 86–93.
Zhidan, Y., Chunming, W., Yanfeng, G., Jing, S., Xiufeng, H., Yuan, L., 2015. Design of a rotary valve orifice for a continuous wave mud pulse generator. Precis. Eng. 41, 111–118.